The nuclear periphery of embryonic stem cells is a transcriptionally permissive and repressive compartment

Li Luo[1,2,*], Katherine L. Gassman[1,*], Lydia M. Petell[1], Christian L. Wilson[1,3], Joerg Bewersdorf[1] and Lindsay S. Shopland[1,‡]

[1]Institute for Molecular Biophysics, The Jackson Laboratory, Bar Harbor, ME 04609, USA
[2]Department of Histology and Embryology, Nanjing Medical University, Nanjing, Jiangsu 210029, China
[3]Department of Mathematics, University of Maine, Orono, ME 04469, USA

*These authors contributed equally to this work
‡Author for correspondence (lindsay.shopland@jax.org)

Accepted 9 August 2009
Journal of Cell Science 122, 3729-3737 Published by The Company of Biologists 2009
doi:10.1242/jcs.052555

Summary

Chromatin adapts a distinct structure and epigenetic state in embryonic stem cells (ESCs), but how chromatin is three-dimensionally organized within the ESC nucleus is poorly understood. Because nuclear location can influence gene expression, we examined the nuclear distributions of chromatin with key epigenetic marks in ESC nuclei. We focused on chromatin at the nuclear periphery, a compartment that represses some but not all associated genes and accumulates facultative heterochromatin in differentiated cells. Using a quantitative, cytological approach, we measured the nuclear distributions of genes in undifferentiated mouse ESCs according to epigenetic state and transcriptional activity. We found that trimethyl histone H3 lysine 27 (H3K27-Me$_3$), which marks repressed gene promoters, is enriched at the ESC nuclear periphery. In addition, this compartment contains 10-15% of chromatin with active epigenetic marks and hundreds of transcription sites. Surprisingly, comparisons with differentiated cell types revealed similar nuclear distributions of active chromatin. By contrast, H3K27-Me$_3$ was less concentrated at the nuclear peripheries of differentiated cells. These findings demonstrate that the nuclear periphery is an epigenetically dynamic compartment that might be distinctly marked in pluripotent ESCs. In addition, our data indicate that the nuclear peripheries of multiple cell types can contain a significant fraction of both active and repressed genes.

Supplementary material available online at
http://jcs.biologists.org/cgi/content/full/122/20/3729/DC1

Key words: Chromatin, Embryonic stem cell, Epigenetics, Nucleus

Introduction

Specific transcription factors and epigenetic marks together regulate gene activity and are crucial for controlling the pluripotent state of ESCs (Spivakov and Fisher, 2007; Lunyak and Rosenfeld, 2008). In addition, the location of a gene within the nucleus also plays an important role in gene activity, although exploration of how the genome is spatially organized within ESC nuclei is only just beginning (Akhtar and Gasser, 2007; Fraser and Bickmore, 2007; Lanctot et al., 2007). One key location in the nucleus is the nuclear periphery, a sub-nuclear compartment that has been shown to alter the expression of associated genes (Andrulis et al., 1998; Finlan et al., 2008; Reddy et al., 2008). This nuclear compartment can repress gene activity and typically accumulates facultative heterochromatin in differentiating mammalian cells (Francastel et al., 2000; Akhtar and Gasser, 2007). However, recent studies in yeast and mammalian cells suggest that at least some active genes also associate with this compartment (Brickner and Walter, 2004; Casolari et al., 2004; Akhtar and Gasser, 2007; Finlan et al., 2008). Hence, the relationship of the nuclear periphery to gene control is still poorly understood, particularly in undifferentiated cells.

A long-standing body of evidence implicates the nuclear periphery in gene repression. Studies in mammalian cell lines have shown that sites of nascent transcription and acetylated histones, which mark transcriptionally active chromatin, are more enriched in the nuclear interior than at the nuclear periphery (Jackson et al., 1993; Sadoni et al., 1999; Bartova et al., 2005). More directly, experimental tethering of genes to the nuclear periphery demonstrated that this compartment can cause transcriptional repression (Andrulis et al., 1998; Finlan et al., 2008; Reddy et al., 2008). However, repression was noted for some but not all tethered genes (Finlan et al., 2008; Kumaran and Spector, 2008). In addition, certain yeast genes move to the nuclear periphery when activated, and in mammalian cells a few 'untethered' expressed genes also preferentially associate with this compartment (Brickner and Walter, 2004; Casolari et al., 2004; Hewitt et al., 2004; Ragoczy et al., 2006; Shopland et al., 2006; Brown et al., 2008; Meaburn and Misteli, 2008). Gene transcription can 'flicker' up and down within a given cell, and direct demonstrations of transcription at the nuclear periphery have only been shown for a few of these mammalian peripheral genes (Shopland et al., 2001; Levsky et al., 2002; Ragoczy et al., 2006; Finlan et al., 2008). The proportion of a mammalian genome that is transcriptionally active and at the nuclear periphery is currently unknown.

Studies in a few mammalian cell types have provided some genome-wide views of the types of chromatin at the nuclear periphery. These sequences are typically later-replicating, correspond to dark Geimsa-staining (G) bands on mitotic chromosomes, and are found in gene-poor regions enriched with repressed genes and genes expressed during embryonic development

(Ferreira et al., 1997; Sadoni et al., 1999; Kupper et al., 2007; Brown et al., 2008; Guelen et al., 2008; Hiratani et al., 2008). However, the complement of genes and the amount of facultative heterochromatin at the nuclear periphery vary among cell types and during cellular differentiation (Francastel et al., 2000; Akhtar and Gasser, 2007). A few genes that move in or out of this compartment, depending on cell type, have been identified, but a genome-wide view of these chromatin dynamics has not been established (Kosak et al., 2002; Zink et al., 2004; Wiblin et al., 2005; Ragoczy et al., 2006; Williams et al., 2006; Hiratani et al., 2008; Meaburn and Misteli, 2008).

Whereas chromatin of the nuclear periphery is enriched with developmentally expressed genes and has been examined in a few differentiated cell lines, little is known about the nuclear periphery of undifferentiated cells. Some markers of facultative and constitutive heterochromatin might accumulate at the nuclear periphery of early embryonic and cultured pluripotent cells, although these were not quantitatively analyzed or compared to active chromatin (Peters et al., 2003; Puschendorf et al., 2008; Terranova et al., 2008). Moreover, in ESCs, chromatin structure is relatively distinct. Histones exchange more rapidly, and transcriptionally active loci are more abundant in ESCs than in differentiated cells (Meshorer et al., 2006; Efroni et al., 2008). ESCs also have a distinct set of so-called bivalent genes, which have epigenetic signatures that include both activating and repressive covalent histone modifications (Azuara et al., 2006; Bernstein et al., 2006; Mikkelsen et al., 2007; Pan et al., 2007; Zhao et al., 2007; Mohn et al., 2008; Cedar and Bergman, 2009). Many of these genes are poised for expression after differentiation (Guenther et al., 2007; Stock et al., 2007). In addition, the composition of the nuclear lamina, a network of intermediate filaments associated with chromatin and the nuclear envelope, differs between ESCs and differentiated cells. In differentiated cells, the nuclear lamina typically contains both B- and A-type lamins, whereas only B-type lamins are present in ESCs and early mouse embryos (Sullivan et al., 1999; Constantinescu et al., 2006; Dechat et al., 2008; Butler et al., 2009). Therefore, the chromatin composition and the amount of transcriptional activity at the ESC nuclear periphery might differ substantially from differentiated cells.

Here, we directly and quantitatively investigate the chromatin contents of the ESC nuclear periphery, both in terms of epigenetic signatures and transcriptional status. We focused on epigenetic marks that have been poorly characterized in situ but define a distinct gene expression program in pluripotent mouse ESCs. To precisely measure the nuclear locations of active and repressed genes in ESC nuclei, we developed a 3D-image analysis tool that maps genomic loci according to the contour of the nuclear edge, including invaginations of the nuclear envelope. This approach allowed us to compare chromatin distributions among ESCs and more differentiated cells. We found that the nuclear peripheries of mouse ESCs and two differentiated cell types contain substantial fractions of both repressed and active genes. Surprisingly, these cell types do not differ in the peripheral fraction of active genes but in repressed genes marked by histone H3 trimethylated on lysine 27 (H3K27-Me_3), which is significantly higher in ESCs. Our findings indicate that active genes at the nuclear periphery are common in some cell types, and that the epigenetic signature of chromatin at the nuclear periphery is dynamic. Further, they suggest a higher level of functional complexity for the nuclear periphery of mammalian cells than previously thought, and point to a specialized function in pluripotent cells.

Results

Repressive and active epigenetic marks localize to the ESC nuclear periphery

To examine the epigenetic state of protein-coding genes at the ESC nuclear periphery, we immunolabeled mouse E14 ESCs with antibodies raised against covalent histone modifications typically found on transcriptionally active and repressed genes (Spivakov and Fisher, 2007; Lunyak and Rosenfeld, 2008). These antibodies recognize histone H3 trimethylated on lysine 4 (H3K4-Me_3) or on lysine 36 (H3K36-Me_3), which accumulate on the promoters and transcribed regions of active genes, respectively. Repressed gene promoters were detected with an antibody against H3K27-Me_3. This modification accumulates on promoters of silenced genes and bivalent genes, which are also marked by H3K4-Me_3 (Azuara et al., 2006; Bernstein et al., 2006; Mikkelsen et al., 2007; Pan et al., 2007; Zhao et al., 2007; Mohn et al., 2008; Cedar and Bergman, 2009). In general, bivalent genes in ESCs are poised for expression or are expressed at greatly reduced levels, and their coding regions do not accumulate H3K36-Me_3 or the elongating form of RNA polymerase II that is phosophorylated on serine 2 of the C-terminal domain (POLII-Ser2-*P*) (Guenther et al., 2007; Stock et al., 2007). Western blotting and immunofluorescence in the presence of competitor peptides demonstrated that the antibodies for these histone modifications recognize the correct target (supplementary material Fig. S1). In addition, two-color immunofluorescence confirmed a greater colocalization of H3K4-Me_3 and H3K36-Me_3 than of H3K27-Me_3 with POLII-Ser2-*P* (supplementary material Fig. S2; Table S1).

Immunostaining ESCs for each of the three epigenetic marks revealed hundreds of concentrated foci throughout the nucleus (Fig. 1A-F). In general, H3K4-Me_3 and H3K36-Me_3 signals appear denser in the nuclear interior, although some foci are detected at or near the outermost edge of the nucleus (Fig. 1A-D, arrows). By contrast, H3K27-Me_3 signals on average are more concentrated around the nucleoli and at the nuclear periphery (Fig. 1E,F). In many cells, H3K27-Me_3 forms a full or partial rim at the edge of the nucleus (Fig. 1F, arrows). These observations suggest that the nuclear periphery of mouse ESCs contains many repressed genes (H3K27-Me_3) as well as active genes (H3K4-Me_3 and H3K36-Me_3). To determine the proportions of active and repressed genes on average at the ESC nuclear periphery, we modified a custom-made 3D-image analysis program, Erosion (Bewersdorf et al., 2006). Erosion precisely maps the positions of nuclear objects relative to the nuclear edge, here defined by DNA counterstain and the presence of lamin B1, a part of the ESC nuclear lamina associated with the nuclear envelope (Gruenbaum et al., 2005). Erosion generates a series of nested 3D-image masks, or shells, shrunk at equal intervals from the nuclear edge (Fig. 1G). Erosion-style analyses such as this are particularly well suited for measuring distances between objects and the nuclear edge (Ronneberger et al., 2008). This approach also takes into account irregular, non-spherical nuclear shapes, as found in the ESCs examined here, and allows for comparisons between different cell types (supplementary material Fig. S3). Whereas 2D analysis is often appropriate for measurements in spherical nuclei, 3D analysis was required to accurately measure the amounts of chromatin at the periphery of the ellipsoidal ESC nuclei studied here, which have a greater fraction of peripheral surface at the ‘top’ and ‘bottom’ than at the ‘side’. The ellipsoidal shape of these feeder-independent ESCs was not due to flattening of the cells during labeling or mounting but rather reflects their attachment to the culture surface (supplementary material Fig. S3). Although adherent, these ESCs express markers characteristic of pluripotent cells (supplementary material Fig. S3)

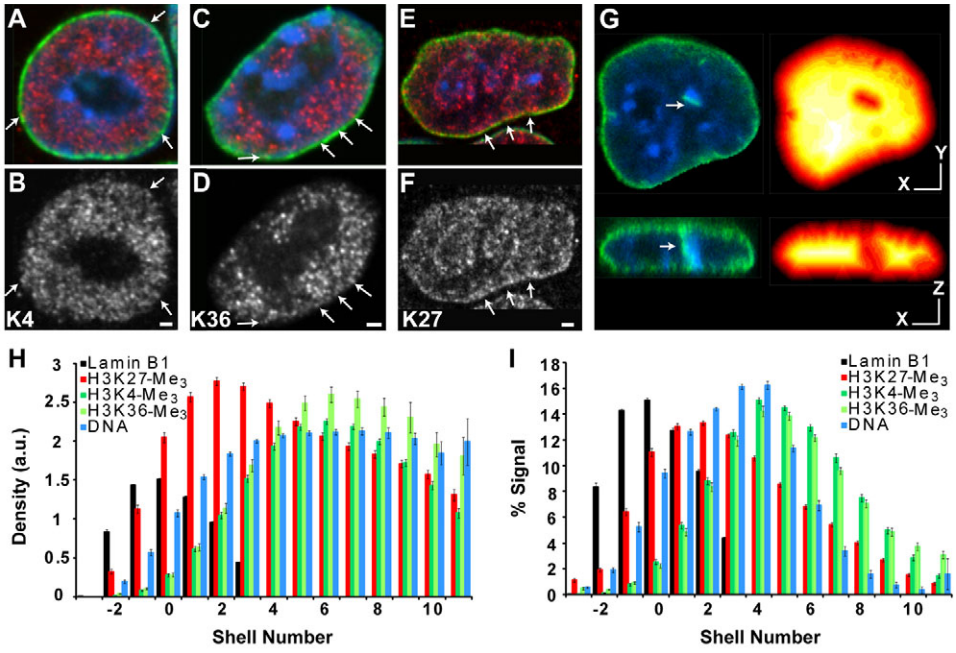

Fig. 1. The ESC nuclear periphery contains epigenetic signatures of both repressed and active genes. (A-D) Immunodetection of H3K4-Me_3 (red in A, white in B) or H3K36-Me_3 (red in C, white in D), found on active genes, indicates hundreds of foci throughout ESC nuclei, including signals (arrows) associated with the nuclear lamina (anti-lamin B1, green). (E,F) H3K27-Me_3 (red in E, white in F), found on repressed promoters, is concentrated at the nuclear periphery and in some regions of the nuclear interior. Arrows indicate a partial rim of H3K27-Me_3 at the nuclear periphery. Nuclei are counterstained with DAPI (blue). Single confocal optical sections are shown. (G) For Erosion analyses, ESCs were stained with anti-lamin B1 (green, left) and DAPI (blue, left) to mark the nuclear edge and invaginations of the nuclear envelope (arrow). 3D image masks with nested 'shells' that follow the contour of the nuclear edge were generated by the Erosion program (red-white, right), which erodes a nuclear edge mask at 200-nm intervals. Optical *X-Y* sections (top) and corresponding sections of *X-Z* projections (bottom) are shown. Scale bars: 1 µm. (H) Erosion analyses of signal density (relative signal intensity per shell volume) indicate that H3K27-Me_3 (red) is most concentrated at the ESC nuclear periphery, indicated by the peak lamin B1 signal (shell 0) (n=108). H3K4-Me_3 (light green) and H3K36-Me_3 (dark green) are more concentrated in the nuclear interior (n=113 and 105, respectively). For comparison, the density distribution of bulk chromatin (blue) was measured from Sytox green counterstaining, which, unlike DAPI, does not preferentially highlight mouse chromocenters. (I) Measurements of the proportions of signals in each nuclear shell show 15% of H3K4-Me_3 and H3K36-Me_3 chromatin within 400 nm of the lamin B1 peak. Relative shell volumes are shown in supplementary material Fig. S4. Lamin B1 relative density is plotted (arbitrary units); axis showing density values is hidden. Error bars are s.e.m. and include variation in shell volume in all density plots.

(Knowles et al., 1978; Yuan et al., 1995). In addition, Erosion masks were in part based on the DNA counterstain, but they did not define the DNA-poor nucleoli as part of the nuclear periphery (Fig. 1G). However, Erosion was modified to use the lamin B1 image to incorporate invaginations of the nuclear envelope into the image masks (Fig. 1G, arrow). These invaginations contain nuclear pores, making them continuous with the cytoplasm and with bone fide parts of the nuclear periphery compartment (Fricker et al., 1997).

ESCs were immunostained to detect one of the three histone modifications and lamin B1 with different fluorescent labels. After DNA counterstaining, cells were imaged by 3D confocal microscopy and evaluated with the Erosion program. For our studies, shells were expanded and then eroded from the nuclear periphery mask at 200-nm intervals. Consistent with our qualitative observations, Erosion analyses indicated a higher density of H3K27-Me_3-tagged chromatin at the ESC nuclear periphery than in the nuclear interior (Fig. 1H). Furthermore, we found 24% of the total H3K27-Me_3 signal within 200 nm of the lamin peak (shells 0 and 1) and 38% within 400 nm (shells 0 to 2), the location where this epigenetic mark was most concentrated (Fig. 1I). By contrast, the distribution of H3K4-Me_3 chromatin differed significantly from that of H3K27-Me_3 [P<0.001, Kolmogorov-Smirnov (KS) test], with a peak density in a more interior nuclear shell. H3K4-Me_3 chromatin was also depleted relative to total DNA at the nuclear periphery, unlike H3K27-Me_3 (Fig. 1H,I). Nonetheless, 8% of the total H3K4-Me_3 signal was within 200 nm of the peak lamin shell, and 17% within 400 nm (Fig. 1I), the shell in which H3K27-Me_3 chromatin was most concentrated. In addition, the measured distribution of H3K36-Me_3 chromatin was similar to H3K4-Me_3 (P>0.5, KS test), further indicating that the periphery contains genes that are actively transcribed as well as repressed (Fig. 1H,I).

Specific expressed genes and gene 'deserts' detected at the ESC nuclear periphery

Because the detection of numerous foci of active chromatin at the nuclear periphery was somewhat unexpected, we sought to verify that these epigenetic marks indeed represent active genes. We first used fluorescence in situ hybridization (FISH) to examine the nuclear location of genes known to be expressed in ESCs. A 4.3 Mb gene-poor region (4 genes/Mb) of mouse chromosome 14 (MMU14) contains multiple genes that are expressed in ESCs and NIH-3T3 fibroblasts (Fig. 2A) (Shopland et al., 2006). The location of the MMU14 region within ESC nuclei is unknown. However, this region was previously found to be enriched at the nuclear periphery of NIH-3T3 cells, making it a good candidate for our study (Shopland et al., 2006). We mapped the locations of two active MMU14 region loci in ESC nuclei. One locus includes the expressed genes *Slain1* and *Sce1* and the other includes *Ndfip2* and *Rbm26* (Fig. 2A). These loci were differentially labeled by two-color FISH in the same ESCs to compare their positions directly. Hybridized cells were subsequently immunostained with anti-lamin B1 antibody, counterstained with DAPI, and imaged by 3D confocal microscopy. The 3D images indicated that both loci are positioned at or adjacent to the nuclear lamina in the majority of cells (Fig. 2B,C). Although these loci are 1.5 Mb apart on MMU14, they can be separated by >1 µm in the nucleus and thus do not necessarily constrain each other to localize to the same nuclear compartment (Fig. 2B, arrows) (Lawrence et al., 1990; Shopland et al., 2006).

Erosion analyses of 3D images confirmed that the expressed MMU14 loci frequently position near the periphery of ESC nuclei (Fig. 2D). Both loci are most often found in the first or second shells adjacent to the peak of the lamin B1 signal, where H3K27-Me_3 also peaks (Fig. 1J,K). Furthermore, approximately 15% of the MMU14 loci map to the shell containing the most concentrated

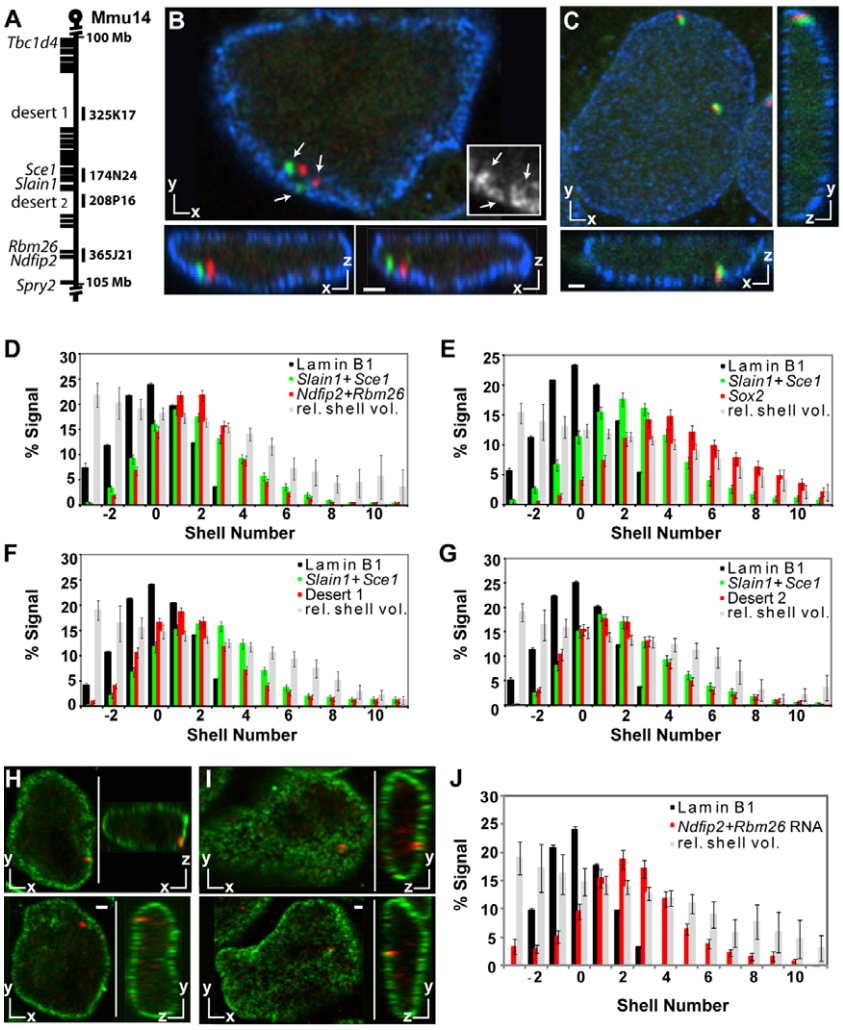

Fig. 2. Transcribing MMU14 loci associate closely with the nuclear periphery. (A) Map of genes (black bars, left) and gene 'deserts' in the MMU14 region under study. *Sce1*, *Slain1*, *Rbm26* and *Ndfip2* are expressed in E14 ESCs (Shopland et al., 2006). BACs used for FISH probes are indicated on the right. (B,C) Two-color FISH detects *Sce1* and *Slain1* (green) and *Rbm26* and *Ndfip2* (red) near the lamina (blue) of ESCs. The cell in B shows three of these four loci (arrows) contacting the lamina (inset, white). Loci from the same chromosome are separated by approximately 1 μm. An *X-Y* optical section and sections from *X-Z* projections are shown. For the cell in C, a maximum *X-Z* projection and single *X-Z* and *Y-Z* sections are shown. (D) 3D distributions of *Sce1*and *Slain1* (green), *Rbm26* and *Ndfip2* (red), and LMNB1 (black) were measured by Erosion for 97 ESCs. Both active loci are most often 200-400 nm from the peak lamin signal. (E) MMU14 gene positions (green) contrast with that of active *Sox2* (red) on MMU3 (n=93). (F,G) MMU14 gene positions (green) are similar to those of two MMU14 gene deserts (red; n=97 and 99, respectively). In D-G, mean shell volumes relative to the total nuclear volume are shown (gray, arbitrary units). (H,I) RNA-FISH detects *Rbm26* and *Ndfip2* transcripts (red) adjacent to the nuclear lamina (anti-LMNB1, green) in two ESC nuclei. Single *X-Y*, *X-Z* and *Y-Z* sections of both FISH signals in each cell are shown as indicated. Scale bars: 1 μm. (J) Erosion analysis of 93 ESCs shows a peak of *Rbm26* and *Ndfip2* transcript signal 400 nm from the lamina, similar to the locus probed by DNA-FISH (D). Error bars, s.e.m.

lamin B1 signal, indicating that they can position very close (< 200 nm) to the nuclear envelope.

The two expressed MMU14 loci have similar nuclear distributions (P>0.5, KS test). By contrast, the distribution of the active MMU3 locus *Sox2*, which previously has been mapped to the ESC nuclear interior, differs significantly from the MMU14 locus *Slain1/Sce1* (P<0.001, KS test) (Fig. 2E) (Williams et al., 2006). These findings indicate that not all active genes have equal access to the nuclear periphery compartment, and that the presence of active chromatin at the ESC nuclear periphery is not simply due to chromatin mobility. The expressed MMU14 locus was also compared to two nearby MMU14 sequences in gene 'deserts', which are depleted of annotated exons and in human cells are enriched in the fraction of lamin-associating chromatin (Ovcharenko et al., 2005; Shopland et al., 2006; Guelen et al., 2008). We find that the MMU14 gene deserts have nuclear distributions similar to those of the active MMU14 genes examined here (P>0.5, KS test) (Fig. 2F,G). Thus, gene deserts as well as some expressed genes localize close to the nuclear edge in mouse ESCs.

MMU14 genes are transcribed at the nuclear periphery

Erosion measurements indicated that approximately 55% of the signal from the expressed MMU14 loci examined is near the ESC nuclear periphery (shells –2 to 2) (Fig. 2D). A similar peripheral fraction was also reported in NIH-3T3 fibroblasts (Shopland et al., 2006). Whereas these data might suggest that at least some genes are transcribed when at the nuclear periphery, many active genes are not continuously transcribed. Rather, transcription can 'flicker' up and down at a given locus when examined on a cell-by-cell basis (Shopland et al., 2001; Levsky et al., 2002). Thus, it was not clear whether the MMU14 genes are transcribed when they localize to the nuclear periphery or only when in more interior portions of the nucleus.

To determine where MMU14 genes are transcribed in the ESC nucleus, we used RNA-FISH to detect the transcribing *Ndfip2*/*Rbm26* locus (Fig. 2H-J). We typically observed two focal accumulations of *Ndfip2*/*Rbm26* transcripts, many of which localize near the ESC nuclear lamina (Fig. 2H,I). Erosion analysis of RNA-FISH samples confirmed these findings, showing a peak of signal at 400 nm from the nuclear lamina and approximately 10% of signal in the peak lamin shell (Fig. 2J). Therefore, these genes can be at the nuclear periphery when transcribed. Furthermore, the distribution of RNA-FISH signals is similar to that of DNA-FISH signals (P>0.5, KS test), suggesting that localization to the periphery is not favored by loci in the 'flickered off' state, but rather that these genes in either state have similar access to this compartment.

Hundreds of active transcription sites localize to the ESC nuclear periphery

As another, more genome-wide measure of transcriptional activity at the ESC nuclear periphery, we examined the locations of the

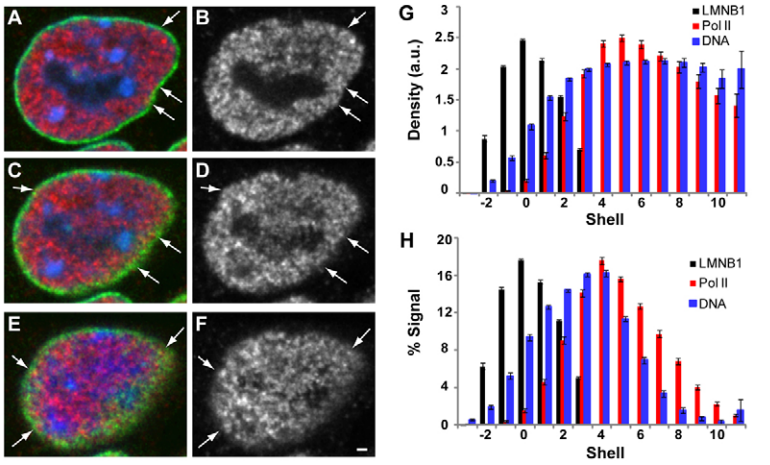

Fig. 3. The ESC nuclear periphery contains multiple transcription sites. (A-F) Three confocal sections of an ESC stained with anti-POLII-Ser2-*P* antibody (red in A,C,E; white in B,D,F) indicate sites of active transcription throughout the nucleus. Examples of transcriptions sites at the nuclear lamina (green) are indicated by arrows. Optical sections shown are separated by 800 nm in the *Z*-axis. Scale bar: 1 μm. (G) Erosion analysis of 102 ESCs indicates a peak density of POLII-Ser2-*P* (red) 1.0 μm from the nuclear lamina (black). (H) 16% of these transcription sites are within 400 nm of the nuclear lamina. Total chromatin distributions based on Sytox green stain (blue) are shown for comparison. Relative shell volumes are shown in supplementary material Fig. S4. Error bars, s.e.m.

elongating form of RNA polymerase II, phosophorylated on serine 2 of its C-terminal domain (POLII-Ser2-*P*) (Kobor and Greenblatt, 2002). POLII-Ser2-*P* transcription sites were then mapped by 3D imaging and Erosion analysis (Fig. 3). POLII-Ser2-*P* was detected throughout the ESC nucleus, appearing more concentrated in the nuclear interior (Fig. 3A-F), consistent with previous observations in other cell types (Jackson et al., 1993; Sadoni et al., 1999). However, multiple POLII-Ser2-*P* transcription sites also were detected in close association with the nuclear lamina (Fig. 3A-F, arrows) (Wansink et al., 1993). These transcription sites were spaced throughout the nuclear periphery compartment and are therefore likely to represent active genes on multiple chromosomes.

Erosion analyses indicated that the density of POLII-Ser2-*P* transcription sites at the ESC nuclear periphery was 20-50% of the density at the nuclear interior (Fig. 3G). Nonetheless, we measured 7% of the total active transcription sites within 200 nm of the peak lamin shell, and 16% within 400 nm (Fig. 3H). Within the peripheral 200 nm region, we counted an average of 909±165 POLII-Ser2-*P* foci per cell. These data confirm our findings using active epigenetic marks (Fig. 1) and indicate that many sites of active transcription are present at the ESC nuclear periphery.

The nuclear peripheries of different cell types contain distinct epigenetic signatures

To determine whether the relative distributions of active and repressed genes at the nuclear periphery are unique to ESCs, we examined the positions of different histone modifications in two additional cell types. These more differentiated cells included embryo-derived NIH-3T3 fibroblasts and adult primary neuronal stem/progenitor cells (NPCs). NPCs were identified as stem/progenitor cells based on the expression of SOX2 and NESTIN (supplementary material Fig. S3). Likewise, the ESCs used in this study were confirmed to be in an undifferentiated state by SOX2 and SSEA1 immunostaining (supplementary material Fig. S3) (Knowles et al., 1978; Yuan et al., 1995; Zhao et al., 2004). In contrast to ESCs, NIH-3T3 cells have a lower DNA density in the nuclear interior and a relatively higher DNA density at nuclear periphery, forming a more apparent rim around the nuclear edge (Fig. 4B,C). In NPCs, larger accumulations of chromatin were also evident at the nuclear periphery, in addition to a rim of dense chromatin (Fig. 4A).

The nuclear distributions of H3K4-Me_3 and H3K27-Me_3 were measured in NPCs and NIH-3T3 cells. Surprisingly, we found for both cell types that the distributions of H3K4-Me_3 were similar to those in ESCs ($P>0.5$, KS tests) (Fig. 4D-E,H-I,L-O). Furthermore, H3K27-Me_3 was markedly different in the two more differentiated cell types compared to ESCs ($P<0.001$) (Fig. 4F-G,J-K,L-O). H3K27-Me_3 was depleted from the nuclear periphery of these two cell types relative to ESCs, despite the appearance of more concentrated heterochromatic DNA at their nuclear peripheries. H3K27-Me_3 foci were fewer and larger in NPCs, further suggesting a greater degree of clustering in the nuclear interior of this cell type compared to ESCs. In addition, the overall level of H3K27-Me_3 might be lower in these cell types compared with ESCs. Fewer genomic binding sites were detected in NPC chromatin in one study but not in another, leaving this an open question (Mikkelsen et al., 2007; Mohn et al., 2008). Together, these data indicate cell-type-specific distributions of H3K27-Me_3 chromatin, which is most concentrated at the ESC nuclear periphery. In addition, they reveal H3K4-Me_3 chromatin at the nuclear peripheries of three different mouse cell types, all with similar proportions of this active epigenetic mark.

Discussion

Here, we show that the nuclear peripheries of three mammalian cell types contain a substantial fraction of transcriptionally active genes as well as repressed genes. We determined the relative fractions of active and repressed genes in this compartment by developing a quantitative, precise, cytological approach that maps chromatin labels throughout the nucleus relative to the nuclear edge. This approach revealed that in undifferentiated mouse ESCs, the nuclear periphery is enriched with repressed genes but also contains hundreds of transcriptionally active genes. The fraction of epigenetically marked active chromatin at the ESC nuclear periphery is similar to that in two lineage-restricted cell types, suggesting that active chromatin is not necessarily displaced from the nuclear periphery upon differentiation. By contrast, the repressive histone modification H3K27-Me_3 is depleted from the nuclear periphery of the other cell types examined relative to ESCs, indicating a dynamic composition of certain epigenetic marks within this compartment. Thus, rather than simply serving as a silencing compartment, the nuclear periphery of mammalian cells has a complex and tissue-specific relationship to gene activity. Our findings further suggest that the composition of epigenetic marks at the nuclear periphery might distinguish pluripotent genomes from those of more lineage-restricted cells.

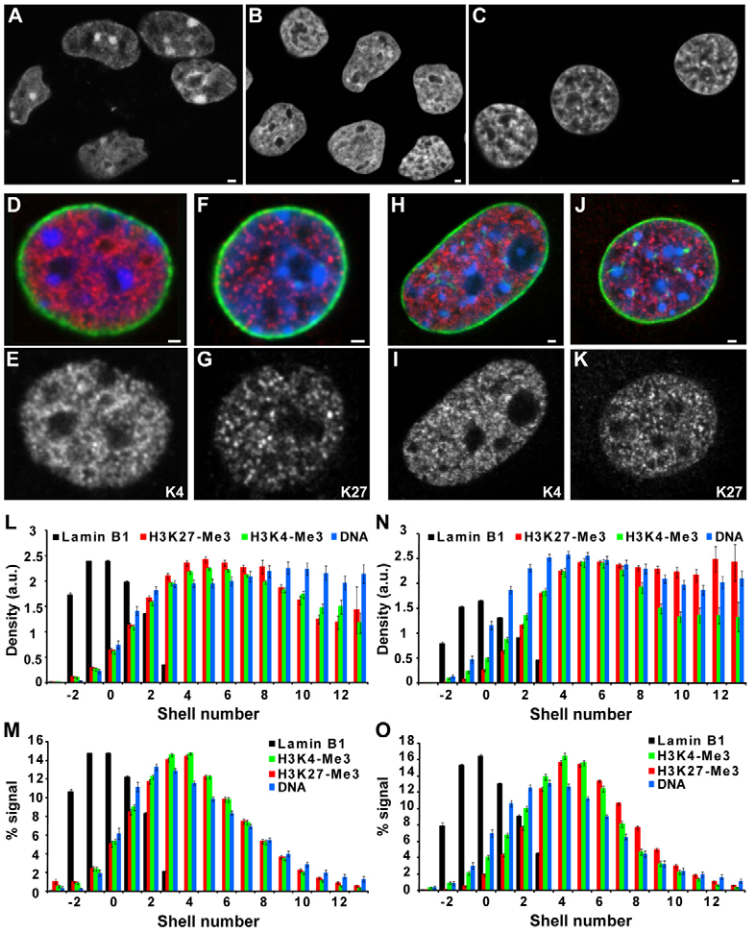

Fig. 4. ESCs chromatin distributions are distinct from NPCs and NIH-3T3 fibroblasts. (A) NPCs, (B) ESCs and (C) NIH-3T3 cells stained with the Sytox green, a DNA dye that does not highlight centromeric heterochromatin. Fewer dense concentrations of DNA are found in ESC nuclei, particularly at the nuclear periphery, compared with the other cell types. (D,E) Immunostaining with anti-H3K4-Me_3 antibody (red in D, white in E) shows signal throughout the NPC nucleus (blue, DAPI), including multiple foci associated with the nuclear lamina (green). A similar distribution was detected in NIH-3T3 cells (H,I). (F,G,J,K) Unlike ESCs, H3K27-Me_3 (red in F and J, white in G and K) is not concentrated at the nuclear periphery of NPCs (F,G) or NIH-3T3 cells (J,K). Single confocal optical sections are shown. Scale bars: 1 μm. (L-O) Erosion measurements indicate similar distributions of H3K27-Me_3 and H3K4-Me_3 in NPCs (n=105 and 106 cells, respectively) (L,M) and in NIH-3T3 cells (n=106 and 91 cells, respectively) (N,O), contrasting with the specific enrichment of H3K27-Me_3 at the ESC nuclear periphery (Fig. 1J,K). Total DNA distributions (blue) are based on Sytox green staining. Relative shell volumes are shown in supplementary material Fig. S4. Error bars, s.e.m.

Quantitative analyses of nuclear periphery chromatin

The nuclear periphery might be a key location for gene expression as well as repression. In addition to providing direct access to nuclear pores, which could enhance RNA export, the nuclear periphery of yeast (*Saccharomyces cerevisea*) has been linked to transcriptional activation and repression, and to changes in chromatin epigenetic state (Blobel, 1985; Hutchinson and Weintraub, 1985; Akhtar and Gasser, 2007). Likewise, repressed genes and a few active genes have been localized to the nuclear periphery of mammalian cells. However, how representative these peripheral active and repressed genes are, relative to the rest of the genomes of unicellular and multicellular organisms, was previously unknown. A quantitative, cytological approach has been needed to measure different types of chromatin genome-wide as well as to compare their nuclear distributions among different cell types.

We have developed a 3D image analysis tool, Erosion, to compare the nuclear distributions of active and repressed chromatin in ESCs and other cell types (Bewersdorf et al., 2006). Because Erosion uses the complete contour of the nuclear edge as a reference, we were able to directly compare cells with different nuclear shapes. Our comparisons revealed similar proportions of H3K4-Me_3 chromatin but different proportions of H3K27-Me_3 at the nuclear peripheries of different cell types. For these studies, we improved upon earlier erosion-style analyses by adapting our program to take into account invaginations of the nuclear envelope. As previously reported, we found cell-type-specific differences in the number of nuclear envelope invaginations, with NIH-3T3 cells containing the most and NPCs the least (Fricker et al., 1997). Without including nuclear envelope invaginations in the Erosion masks, we would have underestimated the fractions of signals near the nuclear envelope in NIH-3T3 fibroblasts relative to the other cell types examined. Therefore, this Erosion feature was crucial to our study.

Because the labeling methods used in this study required the fixation of chromatin in situ, the resulting Erosion measurements represent average nuclear positions of different genomic loci in a population of cells. These averaged positions necessarily reflect the range of motion for each individual locus examined. However, chromatin mobility was not directly assessed in this study, and it is unclear whether chromatin mobility resembles that of more differentiated mammalian cells (Levi et al., 2005; Chuang et al., 2006). Of note, the average fractions of active and repressed chromatin that we measured at the nuclear periphery are probably under- and over-estimates, respectively, because Erosion uses intensity-based thresholding (Materials and Methods). This method over-represents brighter fluorescence signals relative to weaker signals, such as the weaker H3K4-Me_3 at the nuclear periphery and H3K27-Me_3 in the nuclear interior of ESCs.

In addition to relative distributions, Erosion analyses provided measurements of absolute distance to the nuclear periphery, important for determining whether nuclear locations are biologically relevant on a macromolecular scale (Lawrence and Clemson, 2008). Both repressed and active genes were found within 200 nm of the ESC nuclear lamina. This distance approaches the span of large macromolecular complexes. For example, it is approximately twice the length of the nuclear pore basket (Kiseleva et al., 2004). Indeed, genomic loci with active and repressed epigenetic marks

have been recently shown to interact with nuclear porins in one human cell line (Brown et al., 2008). Our measurements in ESCs and two other mouse cell lines support these findings, and strongly suggest that the nuclear periphery of many mammalian cell types contain both transcriptionally active and repressed genes.

Transcriptionally active chromatin at the ESC nuclear periphery

Our measurements indicate higher concentrations of H3K4-Me_3, H3K36-Me_3, and POLII-Ser2-*P* in the nuclear interior, which is consistent with other markers of transcription sites and active chromatin that have been examined previously in non-pluripotent cell lines (Jackson et al., 1993; Sadoni et al., 1999; Bartova et al., 2005). However, because we used quantitative methods, we also found that approximately 10% of transcriptionally active chromatin localizes to the nuclear periphery in ESCs, as well as in two other cell lines. In ESCs, this fraction represents several hundred genes, and possibly more because confocal microscopy cannot resolve very closely positioned genes (Iborra et al., 1996). We have further found that this active peripheral chromatin in ESCs includes a gene-poor region of MMU14 that is enriched with developmental genes. Interestingly, the MMU14 locus *Slain1* is expressed in mouse ESCs but is repressed in NIH-3T3 cells, whereas this region is associated with the nuclear periphery in both cell types (Shopland et al., 2006). These findings suggest that the developmental regulation of these genes, both activation and repression, might occur in association with this compartment.

Consistent with our findings, transcriptionally active chromatin has been detected at the nuclear periphery in a few previous studies. Early electron microscopy of rat hepatocyte nuclei showed nascent transcripts at the edges of peripheral chromatin, although their abundance was not quantified (Nash et al., 1975; Fakan, 1994). The presence of bromo-UTP-labeled transcription sites at the nuclear periphery of two human cell lines has also been noted (Wansink et al., 1993). Similarly, a handful of expressed human and mouse genes detected by FISH are enriched at the nuclear periphery (Hewitt et al., 2004; Ragoczy et al., 2006; Shopland et al., 2006; Brown et al., 2008; Meaburn and Misteli, 2008). In addition, 'tethering' experiments have indicated that not all genes targeted to the nuclear periphery are repressed (Finlan et al., 2008; Kumaran and Spector, 2008). However, very few of these genes have been directly shown to be transcribed when associated with this compartment (Ragoczy et al., 2006; Finlan et al., 2008; Kumaran and Spector, 2008). Thus, our data extend these previous findings by directly demonstrating the transcription of specific native (untethered) genes at the nuclear periphery. Furthermore, earlier studies have not provided a measure of the fraction of transcriptionally active chromatin throughout the genome that is associated with the nuclear periphery. Our approach of labeling active loci genome-wide by fluorescence-based 3D methods in situ has made such measurements possible.

Dynamic epigenetic signature of repressed genes at the nuclear periphery

In addition to epigenetic marks of transcriptionally active chromatin, we also measured the nuclear distributions of epigenetic marks on repressed genes, which have been minimally characterized in situ to date (Peters et al., 2003; Shumaker et al., 2006; Puschendorf et al., 2008; Terranova et al., 2008). By identifying repressed gene promoters based on the H3K27-Me_3 epigenetic mark, we find that these genes are enriched at the nuclear periphery of ESCs. These findings are consistent with the localization of H3K27-Me_3 reported for mouse zygotes and early embryos (Puschendorf et al., 2008; Terranova et al., 2008). Interestingly, in the more differentiated cells examined here, we find that H3K27-Me_3 is not enriched at the nuclear periphery. These data suggest either that H3K27-Me_3 loci move out of this compartment during differentiation, or that H3K27-Me_3 is removed from peripheral chromosomal loci. Indeed, existing evidence supports both mechanisms. Specific mammalian genes have been shown to move towards or from the nuclear periphery in differentiating ESCs and other cell types, probably playing a role in the redistribution of the epigenetic marks we report here (Kosak et al., 2002; Zink et al., 2004; Wiblin et al., 2005; Ragoczy et al., 2006; Williams et al., 2006; Hiratani et al., 2008; Meaburn and Misteli, 2008). In addition, epigenetic marks on individual genes are also known to change. Genes with bivalent marks in ESCs tend to lose either H3K27-Me_3 or H3K4Me_3 in more differentiated, lineage-committed cells, such as the NPCs examined here (Azuara et al., 2006; Mikkelsen et al., 2007; Mohn et al., 2008; Cedar and Bergman, 2009).

The distinct accumulation of H3K27-Me_3 at the nuclear periphery of ESCs raises the intriguing possibility that this compartment contributes to the epigenetic state of pluripotent genomes. Indeed, components of the yeast nuclear periphery play a direct role in gene expression and repression, where some nuclear-porin-associated genes adapt an epigenetic state that leaves them poised for future activation; a state reminiscent of mammalian bivalent genes (Akhtar and Gasser, 2007; Brickner et al., 2007; Stock et al., 2007). In ESCs, H3K27-Me_3 is found primarily on bivalent genes (Mikkelsen et al., 2007; Pan et al., 2007; Zhao et al., 2007; Mohn et al., 2008). Whether bivalent genes are indeed enriched and regulated at the nuclear periphery of mouse ESCs awaits future direct investigation.

The nuclear periphery as a complex but organized compartment

Associations between specific yeast genes and distinct nuclear membrane proteins suggest that genomic sequence is organized *within* the nuclear periphery compartment. It has been proposed that yeast loci form different microdomains next to nuclear pores and other nuclear membrane structures according to the transcriptional activity or epigenetic state (Akhtar and Gasser, 2007). Our data from mammalian cells are consistent with this model; both active and repressed epigenetic marks are at the nuclear periphery and appear as small, discrete foci. By dual-color immunostaining, we detected small-scale domains of repressed loci that are primarily interspersed with POL II-Ser2-*P* in this compartment (supplementary material Fig. S2). Moreover, using FISH, we have previously found that small clusters of genes and interspersed gene deserts on MMU14 can be simultaneously associated with the nuclear envelope (Shopland et al., 2006). Whether these different regions specifically align with nuclear pores or other structures in the nuclear envelope is currently unknown. Nevertheless, their close proximity to the nuclear envelope lends new support to the decades-old hypothesis that the nuclear periphery, with its many direct connections to the cytoplasm, might be a prime location for some genes in the nucleus (Blobel, 1985; Hutchinson and Weintraub, 1985).

Materials and Methods

Cell culture

Feeder-independent mouse E14 ESCs were cultured on gelatin-coated plates at 37°C, 8% CO_2 in Glasgow minimal essential medium (GMEM; Sigma-Aldrich) plus 10% fetal bovine serum (FBS; BioWhittaker Lonza), penicillin/streptomycin (Invitrogen), non-essential amino acids (Invitrogen), sodium pyruvate (Invitrogen), and 1000 U/ml leukemia inhibitory factor (LIF; TJL Protein Chemistry Service). NIH-3T3 fibroblasts

were cultured at 37°C, 5% CO_2 in Dulbecco's modified Eagle's medium (DMEM; Invitrogen) plus 10% FBS and penicillin/streptomycin. One day prior to fixation, cells were plated at 50% confluency on glass coverslips (Gold Seal No. 1.5), which were coated with EHS laminin (Invitrogen) for ESCs. Neural stem cells were isolated from postnatal (P0-P8) C57BL6/J telencephalic subventricular zones (SVZ). Briefly, the SVZ region was micro-dissected, dissociated in Accutase, and triturated to make single cell suspensions. Dissociated cells were cultured in modified DMEM:F12 supplemented with B27, penicillin/streptomycin, and 10 ng/ml basic fibroblast growth factor (bFGF) and 20 ng/ml epidermal growth factor (EGF) to form neurospheres. One day prior to fixation, neurospheres were dispersed and plated at 50% confluency on glass coverslips (Gold Seal No. 1.5) coated with poly D-lysine (BD Bioscience).

Immunofluorescence

Cells were fixed in 4% formaldehyde, 1× PBS for 10 minutes, and permeabilized with 0.5% Triton X-100, 1× PBS for 10 minutes. Cells were stained with 1:500 dilution of rabbit anti-H3K4-Me_3 antibody (ActiveMotif), a 1:500 dilution of mouse anti-H3K27-Me_3 (ActiveMotif), a 1:500 dilution of mouse anti-POLII-Ser2-*P* (H5, Covance), a 1:200 dilution of rabbit anti-SOX2 (Millipore), a 1:1000 dilution of mouse anti-SSEA1 (MC-480, Developmental Studies Hybridoma Bank), or a 1:200 mouse anti-NESTIN (rat-401, Millipore), in 1× PBS, 1% BSA at 37°C for 1 hour. For H3K36-Me_3, cells were extracted for 5 minutes in 0.5% Triton X-100 prior to fixation and immunostaining with a 1:500 dilution of rabbit anti-H3K36-Me_3 (Abcam) (Johnson et al., 2000; Tam et al., 2002). Primary antibodies were detected with 1:250 rhodamine (TRITC)-donkey anti-rabbit, TRITC-donkey anti-mouse IgG, FITC-donkey anti-mouse IgM, or TRITC-donkey anti-rat antibodies (Jackson ImmunoResearch) in 1× PBS, 1% BSA. To mark the nuclear periphery, cells also were stained with 1:250 dilution of goat anti-lamin B (M20, Santa Cruz Biotechnology), which primarily detects lamin B1, and Cy3- or Cy5- donkey anti-goat (Jackson ImmunoResearch) or AlexaFluor-488-donkey anti-goat (Invitrogen). Cells were counterstained with 1 ug/ml DAPI (Sigma-Aldrich), or 500 nM Sytox green (Invitrogen) as indicated, and mounted in 5 mM 1,4-phenylenedamine dihydrochloride (Sigma-Aldrich), 90% glycerol, 1× PBS.

Western blotting

Western blots of histones acid extracted from NIH-3T3 cells were probed with a 1:1000 dilution of anti-H3K27-Me_3, 1:1000 dilution of anti-H3K4-Me_3, or 1:1000 dilution of anti-H3K36-Me_3 antibody pre-incubated with 1 μM of the indicated blocking peptides (Abcam) at 4°C overnight according to manufacturer's directions.

Fluorescence in situ hybridization

Probes were generated by nick-translation of BAC DNA with Cy5-dUTP or Cy3-dUTP (GE). BACs are reported in Fig. 1A and were from the Rp23 library, except for Rp24-174N24. BAC Rp23-129D12 was used for *Sox2*. For DNA-FISH, cells were fixed and permeabilized as described (Solovei et al., 2002), then base-hydrolysed to remove RNA, heat denatured, and hybridized with 50 ng of each probe and 10 μg mouse C_0T1 DNA (Invitrogen), salmon sperm DNA (Sigma-Aldrich), and tRNA (Sigma) as described (Tam et al., 2002). For RNA-FISH, cells were extracted and fixed as described (Tam et al., 2002), and then hybridized to probes directly, omitting base hydrolysis and heat denaturation steps to specifically detect transcripts rather than DNA (Xing et al., 1993). Hybridized cells were post-fixed in 4% formaldehyde and immunostained with goat anti-lamin B, counterstained with DAPI, and mounted as above.

Microscopy and image analysis

Images in supplementary material Figs S1-S3 were obtained with a Zeiss Axioplan 200 equipped with a 100× 1.4 NA oil objective lens, as indicated. For all other analyses, samples were imaged with a TCS SP5 confocal microscope (Leica) with a 100× 1.4 NA oil objective lens and an electronic zoom of 2.0, resulting in *X-Y* pixels of 75×75 nm. 3D image stacks were taken at 200-nm steps. Images were cropped to single cells and resampled in the *Z*-axis to generate cubic voxels using a semi-automatic custom-made Python-program, Crop. Crop displays *Z*-projections of 3D data stacks from which a user can manually define regions of interest (ROIs) outlining single cells. The user-defined trace is computationally optimized for best fit and the same ROI is extracted from all original *X-Y* slices in all detection channels of the data stack. The cropped regions are padded by zeros to create rectangular ROIs again and are combined into 3D data stacks for each channel for further use.

The 3D data stacks representing the different detection channels of a single cell were each loaded into a custom-made C-program, Erosion, a modified version of a program used previously (Bewersdorf et al., 2006). Erosion adjusts for chromatic shift between the channels and then generates a set of masks representing nested 3D shells, each representing the nuclear volume with a constant distance from the nuclear boundary. The boundary (including nuclear envelope invaginations) was automatically defined by combining thresholded voxels of the smoothed DAPI channel with thresholded, smoothed lamin B1 voxels into a 3D mask. The mask was expanded in 3D and then retracted ('eroded') at 200-nm intervals until it vanished completely, forming nested shells with defined distances from the nuclear boundary in the process. To measure the positions of nuclear objects and limit the contribution of residual out-of-focus light, particularly in the *Z*-axis, threshold levels were set to include voxels in only the central image plane of the weaker staining objects. Signals above the threshold were then measured within each shell, as were shell volume and the fraction of voxels above background threshold level. This process was repeated for threshold values above and below the original threshold, which indicated that the measured distributions were relatively threshold-independent. Where indicated, the signal density was determined from the ratio of signal-to-shell volume. Curves representing signal were normalized to a sum of 1 over the whole curve, each shell value therefore representing the signal fraction in that shell. Thus, signal and density values were not calibrated. Their absolute values do not represent meaningful quantities, but normalization is constant within each curve, allowing quantitative relative measures to compare values of different shells. For convenience of display, lamin B1 density curves were normalized to match the curve height of the other displayed curves. Distributions obtained from Erosion were compared using two-sided KS tests.

We thank MaryAnn Handel and Robert Burgess for critical reading of this manuscript, Ana Pombo for advice on experiments, Kyuson Yun for NPCs, and The Jackson Laboratory Cell Biology Service for ESCs. SSEA1 monoclonal antibody was obtained from the Developmental Studies Hybridoma Bank developed under the auspices of the NICHD and maintained by The University of Iowa. This work was supported by NSF EPScOR 0132384, NSF MCB 0817787, NIH NCRR INBRE 5P20RR016463-08, and NCI CA034196 grants. Deposited in PMC for release after 12 months.

References

Akhtar, A. and Gasser, S. M. (2007). The nuclear envelope and transcriptional control. *Nat. Rev. Genet.* **8**, 507-517.

Andrulis, E. D., Neiman, A. M., Zappulla, D. C. and Sternglanz, R. (1998). Perinuclear localization of chromatin facilitates transcriptional silencing. *Nature* **394**, 592-595.

Azuara, V., Perry, P., Sauer, S., Spivakov, M., Jorgensen, H. F., John, R. M., Gouti, M., Casanova, M., Warnes, G., Merkenschlager, M. et al. (2006). Chromatin signatures of pluripotent cell lines. *Nat. Cell Biol.* **8**, 532-538.

Bartova, E., Pachernik, J., Harnicarova, A., Kovarik, A., Kovarikova, M., Hofmanova, J., Skalnikova, M., Kozubek, M. and Kozubek, S. (2005). Nuclear levels and patterns of histone H3 modification and HP1 proteins after inhibition of histone deacetylases. *J. Cell Sci.* **118**, 5035-5046.

Bernstein, B. E., Mikkelsen, T. S., Xie, X., Kamal, M., Huebert, D. J., Cuff, J., Fry, B., Meissner, A., Wernig, M., Plath, K. et al. (2006). A bivalent chromatin structure marks key developmental genes in embryonic stem cells. *Cell* **125**, 315-326.

Bewersdorf, J., Bennett, B. T. and Knight, K. L. (2006). H2AX chromatin structures and their response to DNA damage revealed by 4Pi microscopy. *Proc. Natl. Acad. Sci. USA* **103**, 18137-18142.

Blobel, G. (1985). Gene gating: a hypothesis. *Proc. Natl. Acad. Sci. USA* **82**, 8527-8529.

Brickner, D. G., Cajigas, I., Fondufe-Mittendorf, Y., Ahmed, S., Lee, P. C., Widom, J. and Brickner, J. H. (2007). H2A.Z-mediated localization of genes at the nuclear periphery confers epigenetic memory of previous transcriptional state. *PLoS Biol.* **5**, e81.

Brickner, J. H. and Walter, P. (2004). Gene recruitment of the activated INO1 locus to the nuclear membrane. *PLoS Biol.* **2**, e342.

Brown, C. R., Kennedy, C. J., Delmar, V. A., Forbes, D. J. and Silver, P. A. (2008). Global histone acetylation induces functional genomic reorganization at mammalian nuclear pore complexes. *Genes Dev.* **22**, 627-639.

Butler, J. T., Hall, L. L., Smith, K. P. and Lawrence, J. B. (2009). Changing nuclear landscape and unique PML structures during early epigenetic transitions of human embryonic stem cells. *J. Cell Biochem.* **107**, 609-621.

Casolari, J. M., Brown, C. R., Komili, S., West, J., Hieronymus, H. and Silver, P. A. (2004). Genome-wide localization of the nuclear transport machinery couples transcriptional status and nuclear organization. *Cell* **117**, 427-439.

Cedar, H. and Bergman, Y. (2009). Linking DNA methylation and histone modification: patterns and paradigms. *Nat. Rev. Genet.* **10**, 295-304.

Chuang, C. H., Carpenter, A. E., Fuchsova, B., Johnson, T., de Lanerolle, P. and Belmont, A. S. (2006). Long-range directional movement of an interphase chromosome site. *Curr. Biol.* **16**, 825-831.

Constantinescu, D., Gray, H. L., Sammak, P. J., Schatten, G. P. and Csoka, A. B. (2006). Lamin A/C expression is a marker of mouse and human embryonic stem cell differentiation. *Stem Cells* **24**, 177-185.

Dechat, T., Pfleghaar, K., Sengupta, K., Shimi, T., Shumaker, D. K., Solimando, L. and Goldman, R. D. (2008). Nuclear lamins: major factors in the structural organization and function of the nucleus and chromatin. *Genes Dev.* **22**, 832-853.

Efroni, S., Duttagupta, R., Cheng, J., Dehghani, H., Hoeppner, D. J., Dash, C., Bazett-Jones, D. P., Le Grice, S., McKay, R. D., Buetow, K. H. et al. (2008). Global transcription in pluripotent embryonic stem cells. *Cell Stem Cell* **2**, 437-447.

Fakan, S. (1994). Perichromatin fibrils are in situ forms of nascent transcripts. *Trends Cell Biol.* **4**, 86-90.

Ferreira, J., Paolella, G., Ramos, C. and Lamond, A. I. (1997). Spatial organization of large-scale chromatin domains in the nucleus: a magnified view of single chromosome territories. *J. Cell Biol.* **139**, 1597-1610.

Finlan, L. E., Sproul, D., Thomson, I., Boyle, S., Kerr, E., Perry, P., Ylstra, B., Chubb, J. R. and Bickmore, W. A. (2008). Recruitment to the nuclear periphery can alter expression of genes in human cells. *PLoS Genet.* **4**, e1000039.

Francastel, C., Schubeler, D., Martin, D. I. and Groudine, M. (2000). Nuclear compartmentalization and gene activity. *Nat. Rev. Mol. Cell Biol.* **1**, 137-143.
Fraser, P. and Bickmore, W. (2007). Nuclear organization of the genome and the potential for gene regulation. *Nature* **447**, 413-417.
Fricker, M., Hollinshead, M., White, N. and Vaux, D. (1997). Interphase nuclei of many mammalian cell types contain deep, dynamic, tubular membrane-bound invaginations of the nuclear envelope. *J. Cell Biol.* **136**, 531-544.
Gruenbaum, Y., Margalit, A., Goldman, R. D., Shumaker, D. K. and Wilson, K. L. (2005). The nuclear lamina comes of age. *Nat. Rev. Mol. Cell Biol.* **6**, 21-31.
Guelen, L., Pagie, L., Brasset, E., Meuleman, W., Faza, M. B., Talhout, W., Eussen, B. H., de Klein, A., Wessels, L., de Laat, W. et al. (2008). Domain organization of human chromosomes revealed by mapping of nuclear lamina interactions. *Nature* **453**, 948-951.
Guenther, M. G., Levine, S. S., Boyer, L. A., Jaenisch, R. and Young, R. A. (2007). A chromatin landmark and transcription initiation at most promoters in human cells. *Cell* **130**, 77-88.
Hewitt, S. L., High, F. A., Reiner, S. L., Fisher, A. G. and Merkenschlager, M. (2004). Nuclear repositioning marks the selective exclusion of lineage-inappropriate transcription factor loci during T helper cell differentiation. *Eur. J. Immunol.* **34**, 3604-3613.
Hiratani, I., Ryba, T., Itoh, M., Yokochi, T., Schwaiger, M., Chang, C. W., Lyou, Y., Townes, T. M., Schubeler, D. and Gilbert, D. M. (2008). Global reorganization of replication domains during embryonic stem cell differentiation. *PLoS Biol.* **6**, e245.
Hutchinson, N. and Weintraub, H. (1985). Localization of DNAse I-sensitive sequences to specific regions of interphase nuclei. *Cell* **43**, 471-482.
Iborra, F. J., Pombo, A., Jackson, D. A. and Cook, P. R. (1996). Active RNA polymerases are localized within discrete transcription 'factories' in human nuclei. *J. Cell Sci.* **109**, 1427-1436.
Jackson, D. A., Hassan, A. B., Errington, R. J. and Cook, P. R. (1993). Visualization of focal sites of transcription within human nuclei. *EMBO J.* **12**, 1059-1065.
Johnson, C., Primorac, D., McKinstry, M., McNeil, J., Rowe, D. and Lawrence, J. B. (2000). Tracking COL1A1 RNA in osteogenesis imperfecta. splice-defective transcripts initiate transport from the gene but are retained within the SC35 domain. *J. Cell Biol.* **150**, 417-432.
Kiseleva, E., Allen, T. D., Rutherford, S., Bucci, M., Wente, S. R. and Goldberg, M. W. (2004). Yeast nuclear pore complexes have a cytoplasmic ring and internal filaments. *J. Struct. Biol.* **145**, 272-288.
Knowles, B. B., Aden, D. P. and Solter, D. (1978). Monoclonal antibody detecting a stage-specific embryonic antigen (SSEA-1) on preimplantation mouse embryos and teratocarcinoma cells. *Curr. Top. Microbiol. Immunol.* **81**, 51-53.
Kobor, M. S. and Greenblatt, J. (2002). Regulation of transcription elongation by phosphorylation. *Biochim. Biophys. Acta* **1577**, 261-275.
Kosak, S. T., Skok, J. A., Medina, K. L., Riblet, R., Le Beau, M. M., Fisher, A. G. and Singh, H. (2002). Subnuclear compartmentalization of immunoglobulin loci during lymphocyte development. *Science* **296**, 158-162.
Kumaran, R. I. and Spector, D. L. (2008). A genetic locus targeted to the nuclear periphery in living cells maintains its transcriptional competence. *J. Cell Biol.* **180**, 51-65.
Kupper, K., Kolbl, A., Biener, D., Dittrich, S., von Hase, J., Thormeyer, T., Fiegler, H., Carter, N. P., Speicher, M. R., Cremer, T. et al. (2007). Radial chromatin positioning is shaped by local gene density, not by gene expression. *Chromosoma* **116**, 285-306.
Lanctot, C., Cheutin, T., Cremer, M., Cavalli, G. and Cremer, T. (2007). Dynamic genome architecture in the nuclear space: regulation of gene expression in three dimensions. *Nat. Rev. Genet.* **8**, 104-115.
Lawrence, J. B. and Clemson, C. M. (2008). Gene associations: true romance or chance meeting in a nuclear neighborhood? *J. Cell Biol.* **182**, 1035-1038.
Lawrence, J. B., Singer, R. H. and McNeil, J. A. (1990). Interphase and metaphase resolution of different distances within the human dystrophin gene. *Science* **249**, 928-932.
Levi, V., Ruan, Q., Plutz, M., Belmont, A. S. and Gratton, E. (2005). Chromatin dynamics in interphase cells revealed by tracking in a two-photon excitation microscope. *Biophys. J.* **89**, 4275-4285.
Levsky, J. M., Shenoy, S. M., Pezo, R. C. and Singer, R. H. (2002). Single-cell gene expression profiling. *Science* **297**, 836-840.
Lunyak, V. V. and Rosenfeld, M. G. (2008). Epigenetic regulation of stem cell fate. *Hum. Mol. Genet.* **17**, R28-R36.
Meaburn, K. J. and Misteli, T. (2008). Locus-specific and activity-independent gene repositioning during early tumorigenesis. *J. Cell Biol.* **180**, 39-50.
Meshorer, E., Yellajoshula, D., George, E., Scambler, P. J., Brown, D. T. and Misteli, T. (2006). Hyperdynamic plasticity of chromatin proteins in pluripotent embryonic stem cells. *Dev. Cell* **10**, 105-116.
Mikkelsen, T. S., Ku, M., Jaffe, D. B., Issac, B., Lieberman, E., Giannoukos, G., Alvarez, P., Brockman, W., Kim, T. K., Koche, R. P. et al. (2007). Genome-wide maps of chromatin state in pluripotent and lineage-committed cells. *Nature* **448**, 553-560.
Mohn, F., Weber, M., Rebhan, M., Roloff, T. C., Richter, J., Stadler, M. B., Bibel, M. and Schubeler, D. (2008). Lineage-specific polycomb targets and de novo DNA methylation define restriction and potential of neuronal progenitors. *Mol. Cell* **30**, 755-766.
Nash, R. E., Puvion, E. and Bernhard, W. (1975). Perichromatin fibrils as components of rapidly labeled extranucleolar RNA. *J. Ultrastruct. Res.* **53**, 395-405.
Ovcharenko, I., Loots, G. G., Nobrega, M. A., Hardison, R. C., Miller, W. and Stubbs, L. (2005). Evolution and functional classification of vertebrate gene deserts. *Genome Res.* **15**, 137-145.
Pan, G., Tian, S., Nie, J., Yang, C., Ruotti, V., Wei, H., Jonsdottir, G. A., Stewart, R. and Thomson, J. A. (2007). Whole-genome analysis of histone H3 lysine 4 and lysine 27 methylation in human embryonic stem cells. *Cell Stem Cell* **1**, 299-312.
Peters, A. H., Kubicek, S., Mechtler, K., O'Sullivan, R. J., Derijck, A. A., Perez-Burgos, L., Kohlmaier, A., Opravil, S., Tachibana, M., Shinkai, Y. et al. (2003). Partitioning and plasticity of repressive histone methylation states in mammalian chromatin. *Mol. Cell* **12**, 1577-1589.
Puschendorf, M., Terranova, R., Boutsma, E., Mao, X., Isono, K., Brykczynska, U., Kolb, C., Otte, A. P., Koseki, H., Orkin, S. H. et al. (2008). PRC1 and Suv39h specify parental asymmetry at constitutive heterochromatin in early mouse embryos. *Nat. Genet.* **40**, 411-420.
Ragoczy, T., Bender, M. A., Telling, A., Byron, R. and Groudine, M. (2006). The locus control region is required for association of the murine beta-globin locus with engaged transcription factories during erythroid maturation. *Genes Dev.* **20**, 1447-1457.
Reddy, K. L., Zullo, J. M., Bertolino, E. and Singh, H. (2008). Transcriptional repression mediated by repositioning of genes to the nuclear lamina. *Nature* **452**, 243-247.
Ronneberger, O., Baddeley, D., Scheipl, F., Verveer, P. J., Burkhardt, H., Cremer, C., Fahrmeir, L., Cremer, T. and Joffe, B. (2008). Spatial quantitative analysis of fluorescently labeled nuclear structures: problems, methods, pitfalls. *Chromosome Res.* **16**, 523-562.
Sadoni, N., Langer, S., Fauth, C., Bernardi, G., Cremer, T., Turner, B. M. and Zink, D. (1999). Nuclear organization of mammalian genomes: polar chromosome territories build up functionally distinct higher order compartments. *J. Cell Biol.* **146**, 1211-1226.
Shopland, L. S., Byron, M., Stein, J. L., Lian, J. B., Stein, G. S. and Lawrence, J. B. (2001). Replication-dependent histone gene expression is related to Cajal body (CB) association but does not require sustained CB contact. *Mol. Biol. Cell* **12**, 565-576.
Shopland, L. S., Peterson, K., Lynch, C. R., Thornton, K., Kepper, N., Stein, S., Vincent, S., Molloy, K., Kreth, G., Cremer, C. et al. (2006). Folding and organization of a contiguous chromosome region according to the gene distribution pattern in primary genomic sequence. *J. Cell Biol.* **174**, 27-38.
Shumaker, D. K., Dechat, T., Kohlmaier, A., Adam, S. A., Bozovsky, M. R., Erdos, M. R., Eriksson, M., Goldman, A. E., Khuon, S., Collins, F. S. et al. (2006). Mutant nuclear lamin A leads to progressive alterations of epigenetic control in premature aging. *Proc. Natl. Acad. Sci. USA* **103**, 8703-8708.
Solovei, I., Cavallo, A., Schermelleh, L., Jaunin, F., Scasselati, C., Cmarko, D., Cremer, C., Fakan, S. and Cremer, T. (2002). Spatial preservation of nuclear chromatin architecture during three-dimensional fluorescence in situ hybridization (3D-FISH). *Exp. Cell Res.* **276**, 10-23.
Spivakov, M. and Fisher, A. G. (2007). Epigenetic signatures of stem-cell identity. *Nat. Rev. Genet.* **8**, 263-271.
Stock, J. K., Giadrossi, S., Casanova, M., Brookes, E., Vidal, M., Koseki, H., Brockdorff, N., Fisher, A. G. and Pombo, A. (2007). Ring1-mediated ubiquitination of H2A restrains poised RNA polymerase II at bivalent genes in mouse ES cells. *Nat. Cell Biol.* **9**, 1428-1435.
Sullivan, T., Escalante-Alcalde, D., Bhatt, H., Anver, M., Bhat, N., Nagashima, K., Stewart, C. L. and Burke, B. (1999). Loss of A-type lamin expression compromises nuclear envelope integrity leading to muscular dystrophy. *J. Cell Biol.* **147**, 913-920.
Tam, R., Shopland, L. S., Johnson, C. V., McNeil, J. A. and Lawrence, J. B. (2002). Applications of RNA FISH for visualizating gene expression and nuclear architecture. In *Fish: A Practical Approach* (ed. B. Beatty, S. Mai and J. Squire), pp. 93-118. Oxford: Oxford University Press.
Terranova, R., Yokobayashi, S., Stadler, M. B., Otte, A. P., van Lohuizen, M., Orkin, S. H. and Peters, A. H. (2008). Polycomb group proteins Ezh2 and Rnf2 direct genomic contraction and imprinted repression in early mouse embryos. *Dev. Cell* **15**, 668-679.
Wansink, D. G., Schul, W., VanDerKraan, I., VanSteensel, B., VanDriel, R. and DeJong, L. (1993). Fluorescent labeling of nascent RNA reveals transcription by RNA polymerase II in domains scattered throughout the nucleus. *J. Cell Biol.* **122**, 283-293.
Wiblin, A. E., Cui, W., Clark, A. J. and Bickmore, W. A. (2005). Distinctive nuclear organisation of centromeres and regions involved in pluripotency in human embryonic stem cells. *J. Cell Sci.* **118**, 3861-3868.
Williams, R. R., Azuara, V., Perry, P., Sauer, S., Dvorkina, M., Jorgensen, H., Roix, J., McQueen, P., Misteli, T., Merkenschlager, M. et al. (2006). Neural induction promotes large-scale chromatin reorganisation of the Mash1 locus. *J. Cell Sci.* **119**, 132-140.
Xing, Y., Johnson, C. V., Dobner, P. and Lawrence, J. B. (1993). Differential nuclear distribution of intron and exon sequences for endogenous RNAs revealed by fluorescence in situ hybridization. *Science* **259**, 1326-1330.
Yuan, H., Corbi, N., Basilico, C. and Dailey, L. (1995). Developmental-specific activity of the FGF-4 enhancer requires the synergistic action of Sox2 and Oct-3. *Genes Dev.* **9**, 2635-2645.
Zhao, S., Nichols, J., Smith, A. G. and Li, M. (2004). SoxB transcription factors specify neuroectodermal lineage choice in ES cells. *Mol. Cell Neurosci.* **27**, 332-342.
Zhao, X. D., Han, X., Chew, J. L., Liu, J., Chiu, K. P., Choo, A., Orlov, Y. L., Sung, W. K., Shahab, A., Kuznetsov, V. A. et al. (2007). Whole-genome mapping of histone H3 Lys4 and 27 trimethylations reveals distinct genomic compartments in human embryonic stem cells. *Cell Stem Cell* **1**, 286-298.
Zink, D., Amaral, M. D., Englmann, A., Lang, S., Clarke, L. A., Rudolph, C., Alt, F., Luther, K., Braz, C., Sadoni, N. et al. (2004). Transcription-dependent spatial arrangements of CFTR and adjacent genes in human cell nuclei. *J. Cell Biol.* **166**, 815-825.

Journal of Cell Science